2024

Self-assembling polypeptides in complex coacervation

Arvind Sathyavageeswaran
University of Massachusetts Amherst

Júlia Bonesso Sabadini
University of Massachusetts Amherst

Sarah L. Perry
University of Massachusetts Amherst

Recommended Citation

Sathyavageeswaran, Arvind; Sabadini, Júlia Bonesso; and Perry, Sarah L., "Self-assembling polypeptides in complex coacervation" (2024). *Macromolecules*. 928.
https://doi.org/10.1021/acs.accounts.3c00689

Self-assembling polypeptides in complex coacervation

Arvind Sathyavageeswaran,[†,1] Júlia Bonesso Sabadini,[†,1,2] Sarah L. Perry[1,*]

[†] Equal contributions, * Corresponding author: perrys@engin.umass.edu

[1] Department of Chemical Engineering, University of Massachusetts Amherst, Amherst, MA, 10003, USA

[2] Institute of Chemistry, University of Campinas, (UNICAMP), Campinas, SP, 13083-970, Brazil

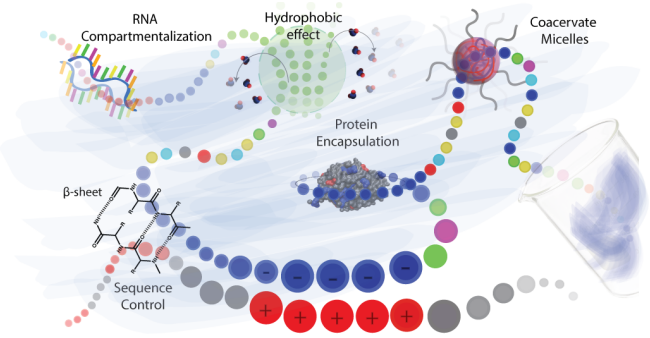

Conspectus:

Intracellular compartmentalization plays a pivotal role in cellular function, with membrane-bound organelles and membrane-less biomolecular 'condensates' playing key roles. These condensates, formed through liquid-liquid phase separation (LLPS), enable selective compartmentalization without the barrier of a lipid bilayer, thereby facilitating rapid formation/dissolution in response to stimuli. Intrinsically disordered proteins (IDPs) and/or proteins with intrinsically disordered regions (IDRs), which are often rich in charged and polar amino acid sequences, scaffold many condensates, often in conjunction with RNA.

Comprehending the impact of IDP/IDR sequences on phase separation poses a challenge due to the extensive chemical diversity resulting from the myriad amino acids and

post-translational modifications. To tackle this hurdle, one approach has been to investigate LLPS in simplified polypeptide systems, which offer a narrower scope within the chemical space for exploration. This strategy is supported by studies that have demonstrated how IDP function can largely be understood based on general chemical features, such as clusters or patterns of charged amino acids, rather than residue-level effects, and the ways in which these kinds of motifs give rise to an ensemble of conformations.

Our lab has utilized complex coacervates assembled from oppositely-charged polypeptides as a simplified material analogue to the complexity of liquid-liquid phase separated biological condensates. Complex coacervation is an associative LLPS that occurs due to the electrostatic complexation of oppositely-charged macro-ions. This process is believed to be driven by the entropic gains resulting from the release of bound counterions and the reorganization of water upon complex formation. Apart from their direct applicability to IDPs, polypeptides also serve as excellent model polymers for investigating molecular interactions due to the wide range of available side-chain functionalities and the capacity to finely regulate their sequence, thus enabling precise control over interactions with guest molecules.

Here, we discuss fundamental studies examining how charge patterning, hydrophobicity, chirality, and architecture affect the phase separation of polypeptide-based complex coacervates. These efforts have leveraged a combination of experimental and computational approaches that provide insight into the molecular level interactions. We also examine how these parameters affect the ability of complex coacervates to incorporate globular proteins and viruses. These efforts couple directly with our fundamental studies into coacervate formation, as such 'guest' molecules should not be considered as experiencing

simple encapsulation and are instead active participants in the electrostatic assembly of coacervate materials. Interestingly, we observed trends in the incorporation of proteins and viruses into coacervates formed using different chain length polypeptides that are not well explained by simple electrostatic arguments and may be the result of more complex interactions between globular and polymeric species. Additionally, we describe experimental evidence supporting the potential for complex coacervates to improve the thermal stability of embedded biomolecules such as viral vaccines.

Ultimately, peptide-based coacervates have the potential to help unravel the physics behind biological condensates while paving the way for innovative methods in compartmentalization, purification, and biomolecule stabilization. These advancements could have implications spanning from medicine to biocatalysis.

Key References:

- Chang, L. W.; Lytle, T. K.; Radhakrishna, M.; Madinya, J. J.; Vélez, J.; Sing, C. E.; Perry, S. L. Sequence and Entropy-Based Control of Complex Coacervates. *Nat. Commun*. **2017**, *8*, 1273.[1] This study employs a combination of experiments, theory, and simulations to explore the fundamental physics underpinning charge patterning effects on the phase behavior of complex coacervates.
- Lytle, T. K.; Chang, L. W.; Markiewicz, N.; Perry, S. L.; Sing, C. E. Designing Electrostatic Interactions via Polyelectrolyte Monomer Sequence. *ACS Cent. Sci*. **2019**, *5*, 709–718.[2] This study expands the mechanistic understanding of charge patterning in complex coacervates through a combination of experiments and computational frameworks.
- Perry, S. L.; Leon, L.; Hoffmann, K. Q.; Kade, M. J.; Priftis, D.; Black, K. A.; Wong, D.; Klein, R. A.; Pierce, C. F.; Margossian, K. O.; Whitmer, J. K.; Qin, J.; de Pablo, J. J.; Tirrell, M. Chirality-Selected Phase Behaviour in Ionic Polypeptide Complexes. *Nat. Commun*. **2015**, *6, 6052*.[3] This study explores the role of chirality in determining the solid vs. liquid state of complex coacervates due to a combination of electrostatic and hydrogen-bonding interactions.
- McTigue, W. C. B.; Perry, S. L. for Encapsulating Proteins into Complex Coacervates, *Soft Matter* **2019**, *15*, 3089-3103.[4] This paper explores the way in which pH, ionic strength, polymer length, and polymer charge density affect the incorporation of various model proteins into a two-polymer coacervate system.

Introduction: Biological Condensates and the Connection to Complex Coacervation

Compartmentalization significantly contributes to cellular function. Intracellular compartments, known as organelles, exist in two forms: membrane-bound vesicles and membrane-less 'condensates'.[5–7] These condensates are the result of liquid-liquid phase separation (LLPS), which enables selective partitioning and compartmentalization without the barrier of a lipid membrane, and have the potential for rapid formation/dissolution in response to stimuli.[8–10]

The ability for condensates to undergo LLPS has largely been associated with intrinsically disordered proteins (IDPs) that are thought to scaffold these structures. IDPs tend to lack a well-defined 3D structure as a result of high concentrations of repetitive sequences of charged and polar residues.[11–13] Many condensates are made of IDPs and RNA (Figure 1a1), and form compartments that sequester biomolecules for use in biochemical reactions.[7,14,15] For example, P granules, which are found in the germ cells of certain organisms, form via complexation between IDPs and RNA and play a crucial role in germ cell development (Figure 1a2).[5,10] For details on the role of IDPs and proteins with intrinsically disordered regions in LLPS, we refer the reader to a selection of papers .[5,6,8,10,11]

While the interactions responsible for the formation of condensates can be highly intricate, electrostatic effects can play a significant role. For instance, Nott *et al*. showed that condensates formed by the self-association of the IDP Ddx4 (Figure 1a3) were primarily driven by electrostatics due to large blocks of alternating charged and polar groups.[15] However, understanding how IDP sequence affects phase separation is challenging due to the vast chemical space created by the number of amino acids and post-translational modifications

available. One strategy to circumvent this challenge has been to study LLPS in simplified polypeptide systems that explore a more limited chemical space.

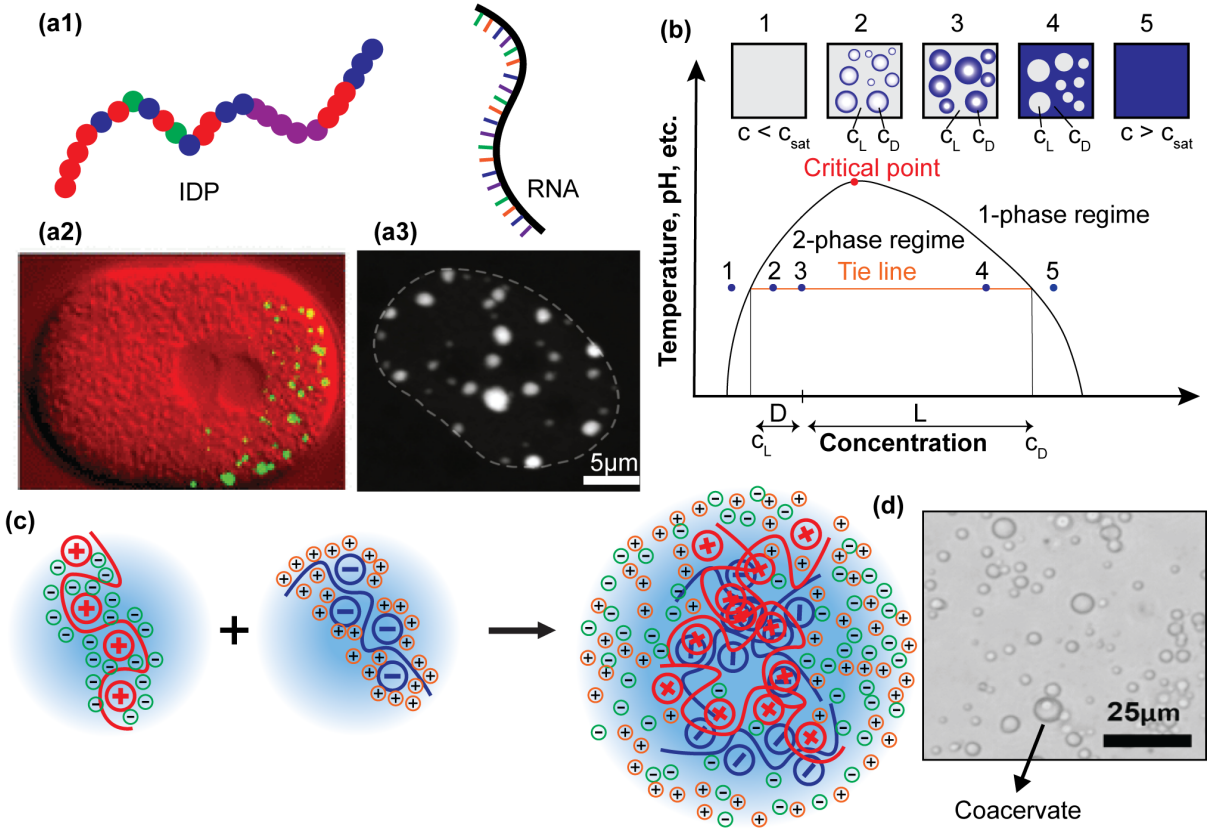

Figure 1: Overview of biomolecular condensates and complex coacervation. (a1) Schematic of an IDP and RNA. **(a2)** Fluorescence micrographs of P granules in a *Caenorhabditis elegans* embryo, adapted with permission from Ref. 16. Copyright 2013 the American Physical Society, and **(a3)** Ddx4 condensates. Reproduced with permission from Ref 15. Copyright The Authors, some rights reserved; exclusive licensee Cell Press. Distributed under a Creative Commons Attribution License 4.0 (CC BY) https://creativecommons.org/licenses/by/4.0/. **(b)** General phase diagram depicting LLPS, adapted from Ref. 17. Phase separation occurs only within the two-phase region, where c_{sat} is the concentration at the boundary of the one-phase and two-phase regions. **(c)** Schematic of oppositely-charged polymers undergoing complex coacervation and releasing condensed counterions. **(d)** Micrograph of a coacervate formed from poly(lysine-co-glycine) and poly(*D,L*-glutamate).

Studies of complex coacervation have proven to be particularly useful for the exploration of electrostatics on LLPS. Complex coacervation is an associative LLPS that involves the electrostatic complexation of oppositely-charged macro-ions, the driving force for which is thought to be the entropic gains associated with the release of bound counterions and the restructuring of water upon complex formation (Figure 1c,d).[18–21] Figure 1b presents a generalized phase diagram for LLPS, illustrating how phase separation can occur as a function of parameters such as temperature, pH, etc., relative to polymer concentration. A

sample prepared at a concentration within the two-phase region splits along a tie-line into a polymer-dense phase and a polymer-poor phase. These phase diagrams are crucial for understanding coacervation, with ionic strength being the most common parameter used to modulate complex coacervation.

Studies of the complex coacervation of relatively simple sequence-controlled polypeptides have proven to be a useful strategy for understanding fundamental aspects of the self-assembly and LLPS of these materials. In addition to their direct relevance to IDPs, polypeptides also represent an ideal model polymer for the study of molecular interactions because of the variety of side-chain functionalities available and the ability to precisely control sequence and therefore interactions with guest molecules.[12,22–24] However, for many simplified sequences (*e.g.*, a binary repeating pattern), it is usually necessary to use solid-phase peptide synthesis,[25,26] rather than protein expression. This caveat means that the materials used in most coacervate studies should be thought of more as polymers (with a molecular weight distribution), than as monodisperse IDPs. Nevertheless, we expect that the trends observed for these 'polymeric' materials should translate reasonably to biological systems.[27]

In this review, we focus on understanding the complex coacervation of polypeptides. Studies have allowed for exploration of sequence effects on electrostatic interactions, in tandem with orthogonal interactions such as 'hydrophobicity' and hydrogen bonding. In addition to our discussion of the 'polymers' in these systems, we will also consider the parallel ways in which interactions facilitate the incorporation of globular proteins and viruses into coacervates. Additionally, we will explain how fundamental knowledge developed in the context of polypeptide-based coacervates allows for understanding the nuances of biological

condensates. For a more focused reading on the biology and biophysics of condensates, and driving forces such as π-π and cation-π interactions, we refer the reader to other reports.[10,28–31]

Peptide Sequence and Phase Separation:

The complex interplay between sequence, structure, and function represents a long-standing challenge for the biological and polymer science communities.[32,33] IDP function is commonly considered with respect to an ensemble of conformations, rather than a single structure. This emphasis on structural ensembles has meant that general chemical features, such as clusters or patterns of charged amino acids, drive the phase separation of IDPs, rather than residue-level effects.[13,34,35]

One well-known example of charge-patterning effects is the intracellular phase separation of the Nephrin intracellular domain (NICD) IDP via complex coacervation.[36] Here, the negatively-charged NICD co-assembled with positively-charged partners, such as RNA/DNA-binding proteins, to form protein-rich liquid droplets. This study highlighted the importance of general patterns of negative and aromatic/hydrophobic residues, rather than the precise sequence, in promoting phase separation, and is just one example of how understanding general sequence features affecting phase separation can affect cellular processes.

To explore the mechanism whereby patterns of charge affect complex coacervation, Chang and Lytle *et al*. combined experimental studies of poly(lysine-co-glycine) in complex with homopolyglutamate, with computational efforts.[1] The cationic polypeptides contained an equal number of lysine and glycine monomers, arranged in regular repeating patterns of different block sizes (Figure 2c). Coacervate experiments were performed using a 1:1 mixture

of cationic and anionic groups (*i.e.,* charge neutrality), meaning that the number of lysine-co-glycine chains was twice that of the polyglutamate.

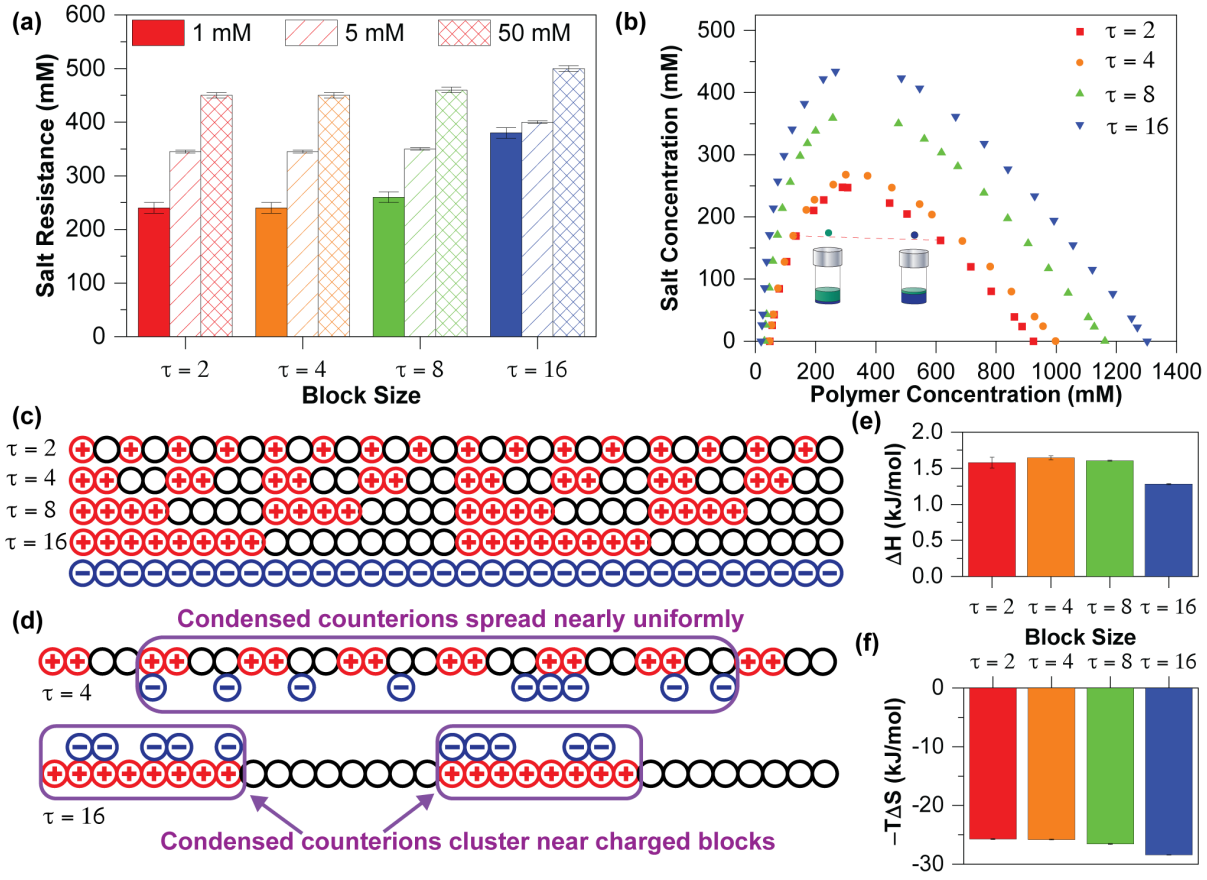

Figure 2: Effect of charge patterning on complex coacervation. (a) Salt resistance vs. charge block size (τ) for charge-patterned coacervates prepared at different concentrations. Error bars reflect the intervals between samples. **(b)** Phase diagrams from simulations as a function of τ. A tie line connecting the coacervate and supernatant phases shows the difference in salt concentration between the two phases. **(c)** Schematic of the block sizes for the polycation and the homopolyanion. **(d)** Schematic of counterion condensation on different sized charged blocks. **(e)** ΔH and **(f)** –TΔS data for the ion pairing step from ITC experiments as a function of blockiness. Reproduced with permission from Ref 1. Copyright The Authors, some rights reserved; exclusive licensee Nature. Distributed under a Creative Commons Attribution License 4.0 (CC BY) https://creativecommons.org/licenses/by/4.0/.

The strength of the interactions between polypeptides, and thus the coacervate phase behavior, was described in terms of stability against salt. Figure 2b shows phase diagrams obtained from coarse-grained simulations as a function of polymer and salt concentration, and polycation sequence.[1] While these binodal curves map out the full extent of the two-phase region, parallel experiments are challenging given the small amounts of material typical when studying polypeptides. Thus, a comparison was made between the calculated binodals and experimentally determined values for the 'salt resistance' at low concentrations of

polymer. Both simulations and salt resistance data showed that the size of the two-phase coexistence region increased with blockiness (i.e., larger values of τ, Figure 2a,b). While one might expect that increased blockiness would increase coacervate stability, it was necessary to look beyond the phase diagrams to understand the molecular underpinnings for this result.

The size of the two-phase region can be correlated to the magnitude of the free energy for phase separation. Therefore, the authors used both experimental and computational approaches to investigate the thermodynamic driving force behind coacervation. Experimentally, isothermal titration calorimetry (ITC) was used to determine the change in free energy for coacervate formation. Coacervation was described using a two-step model where the polymers first undergo 'ion pairing,' described by an enthalpy and a binding constant (which defines a free energy from which an entropy can be calculated), followed by 'coacervation,' where only a heat of phase change is considered.[1,37] This analysis allows for the separation of entropic and enthalpic contributions. Consistent with other reports,[18,37] ITC measurements showed a small, positive enthalpic (ΔH) contribution to ion pairing, with no obvious trends with regards to sequence (Figure 2e). In contrast, the values for –TΔS were energetically favorable, an order of magnitude larger than ΔH, and strengthen with block size (Figure 2f). The enthalpy of phase change was found to be an order of magnitude smaller than ΔH for ion pairing (data not shown).

While one might have expected significant enthalpic contributions due to the role of electrostatics in coacervation,[18] the ITC data confirmed that entropy is the driving force for coacervation – a result consistent with traditional counterion-release explanations for coacervation.[18,37–39] Mechanistically, counterions localize near highly charged polymers to decrease the local electrostatic energy at the expense of counterion translational entropy.[40]

During coacervation, the oppositely-charged polypeptides can self-neutralize, releasing the counterions into solution.

This mechanism can similarly explain the effect of charge patterning on coacervation. In Figure 2d, we consider a schematic of counterion localization around polymers with two different patterns of charge. For polymers with small block sizes, the counterions can distribute relatively uniformly along the chain while still facilitating electroneutrality. However, for blockier sequences, the counterions must cluster more tightly around the charged blocks. This variation in the degrees of freedom available to the bound counterions before complexation with block size directly accounts for the larger gain in entropy observed for coacervates with blockier polypeptides, a result that was also supported by simulations.[1]

The idea that the driving force for coacervation comes from the release of bound counterions means that the phase behavior is largely dictated by the ways in which those counterions cluster around a polymer in solution *before* complexation takes place. Building on their initial work, Lytle and Chang *et al*. delved deeper into the effects of charge patterning, looking at sequences with varying charge fractions (f_c) and average lengths of charged monomer "runs" ($\langle n_r \rangle$), (Figure 3a).[2] Trends in salt resistance (Figure 3b) revealed how sequence and charge fraction can be independently tuned to yield the desired phase behavior. For example, sequences D, I, and F, exhibit similar salt resistances despite having different charge contents.

Figure 3c highlights the critical role that cooperativity between neighboring charges has on phase behavior. The introduction of just a single neutral residue into a run of eight charged lysines has a far more dramatic effect on the salt resistance than subsequent growth of the neutral block. These observations serve as an example of the ways in which only general

trends of composition can dominate LLPS.[36] Furthermore, these same ideas can also be applied to polyampholytes, which have direct relevance to IDPs.[41,42]

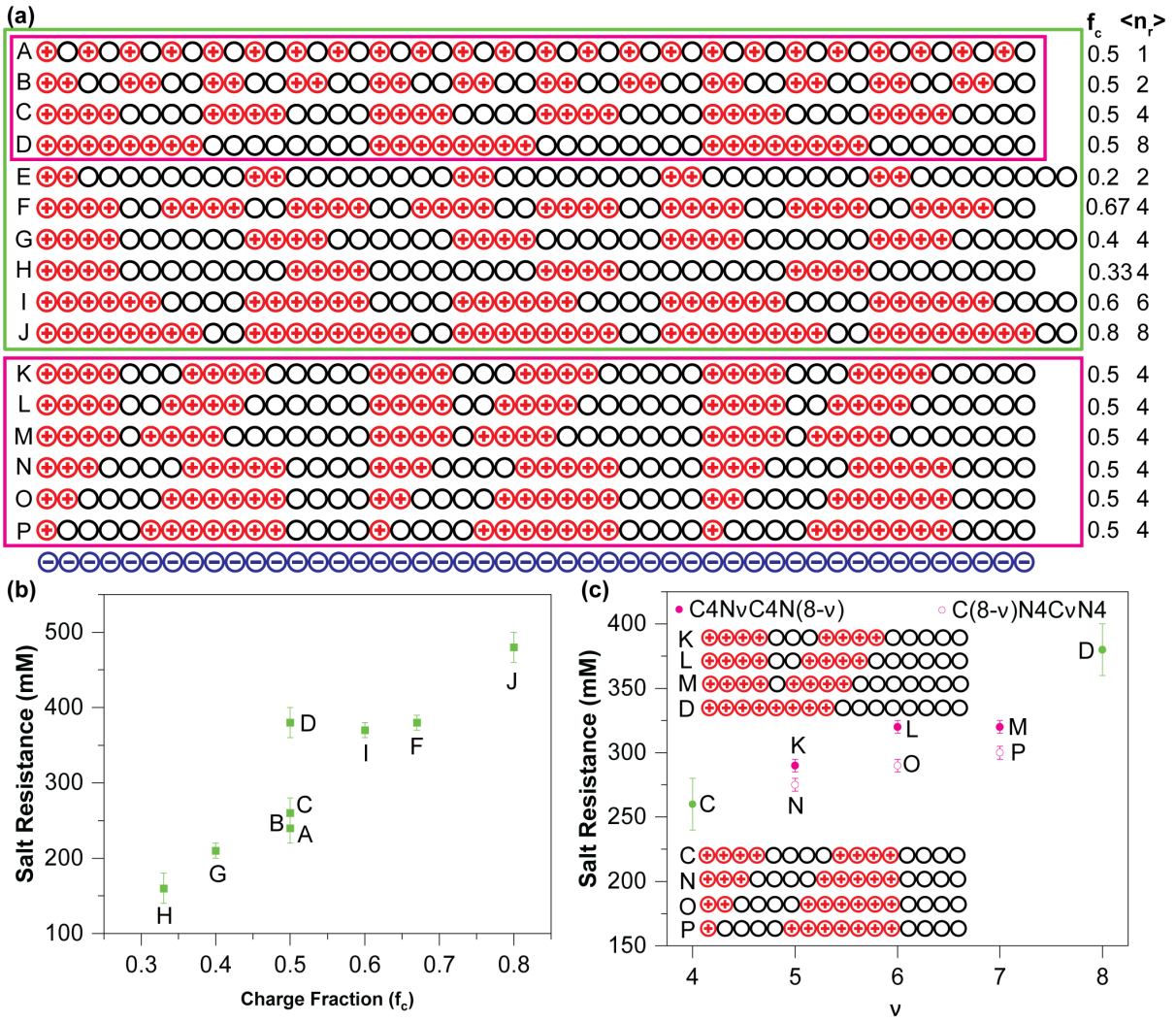

Figure 3: Effect of charge fraction and sequence. (a) Schematic of sequences explored, characterized by the charge fraction f_c and the average "run" length $\langle n_r \rangle$. **(b)** Salt resistance for coacervates formed from the sequences in **(a)**. Data for sequences A-D match the 1 mM data shown in Figure 2a. **(c)** Salt resistance data for sequences with the same f_c and $\langle n_r \rangle$. Sequences K,L,M,D vary the length of neutral spacers, denoted by v and 8-v, between two charge blocks of length four, while C,N,O,P vary the charge block size while holding the neutral block constant at four. Data highlighted in green are at different charge fractions, while those in pink are at f_c = 0.5. Data adapted from Ref. 2.

Charge Density and Hydrophobicity:

Biologically relevant IDPs involve a more complex hierarchy of interactions than simple charge patterning. Expanding this complexity, Leon and coworkers explored the role of both charge density and hydrophobicity.[43] They synthesized sequence-controlled poly(lysine) and poly(glutamate) with two different charge densities (50% and 75%) and

increasingly hydrophobic neutral co-monomers, going from glycine (G) to alanine (A) to leucine (L) (Figure 4a). The resulting coacervates showed increased salt stability with increasing charge density, as expected based on counterion release (Figure 4b). It is worth noting that the magnitude of the salt resistance for the 50% charged glycine-containing system was significantly lower than the values observed by Chang and Lytle *et al*.[1] This difference is due the shorter length polypeptides used in the study by Leon and coworkers and the fact that both polypeptides were patterned.

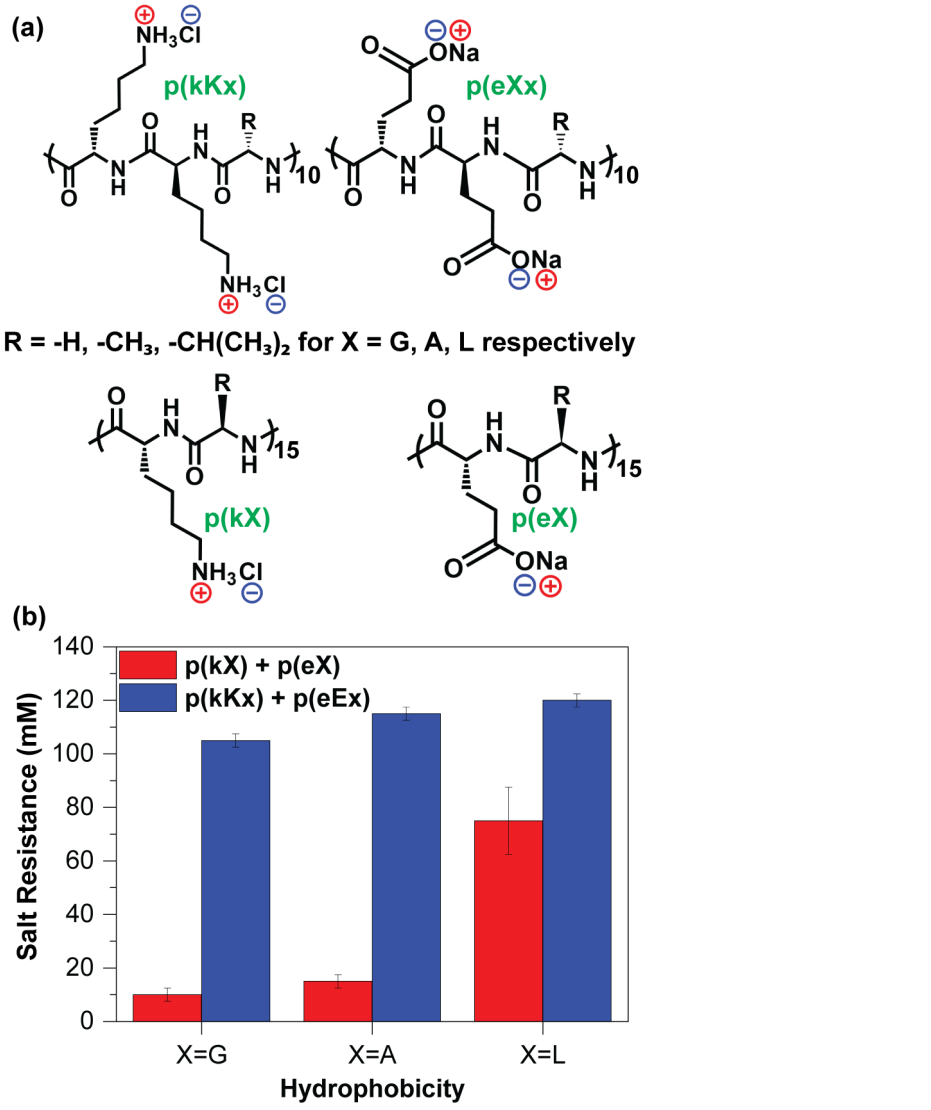

Figure 4: Sequence and hydrophobicity effects. (a) Chemical structures of the polypeptides used in the study. Lowercase single-letter abbreviations represent D-chirality; uppercase represents L-chirality. A discussion of chirality effects is given in the following section. **(b)** Salt resistance as a function of charge density and hydrophobicity. Error bars reflect the interval between samples. Data adapted from Ref. 43.

The coacervates also showed increased salt stability with increasing hydrophobicity (Figure 4b). While qualitatively, one could invoke the idea that the more hydrophobic material is less soluble in water, and therefore 'prefers' to remain in the 'less-hydrated' coacervate phase, the origin of this phenomenon is likely correlated with the structure of water. Changes in the ordering of water around hydrophobic monomers during coacervation could help to increase the entropic driving force (in addition to that of the condensed counterions) and help to enhance the salt stability of the coacervates. The importance of water effects on coacervation has been seen in a number of studies, including those examining the hydrophobicity and the impact of various salts.[19–21,44–47]

Chirality and Hydrogen Bonding:

Thus far, we have focused on the idea of *liquid-liquid* phase separation. However, many IDPs have been correlated with neurodegenerative disease and the formation of solid-like aggregates (*e.g.*, amyloids).[48,49] While IDPs evolved to function at the precipice of solid aggregate formation, most synthetic polypeptides used for complex coacervation must address this issue directly.

Control over the liquid vs. solid state of complexes has been explored with regards to amino acid chirality.[3,50] While most naturally-occurring proteins are composed of *L*-amino acids, complexation between poly(*L*-lysine) and poly(*L*-glutamate) resulted in solid precipitation (Figure 5a). Similarly, complexation between any two homochiral polypeptides, whether composed of *L*- or *D*-amino acids resulted in solid aggregates. Fourier transform infrared spectroscopy demonstrated the presence of β-strand structures, similar to amyloids, resulting from hydrogen bonding between the peptide backbones (Figure 5c).

To achieve liquid coacervates it was necessary for at least one of the polypeptides to be a racemic (50:50) mixture of *D*- and *L*-amino acids (Figure 5a). Interestingly, while the presence of hydrogen bonds resulted in solid precipitation, it was still possible to dissolve these precipitates with salt, though the solid complexes showed a higher stability against salt compared to liquid coacervates (Figure 5b). Additionally, the authors also demonstrated that disruption of hydrogen bonding via the addition of urea allowed for 'melting' of the solid precipitates into a coacervate-like liquid.

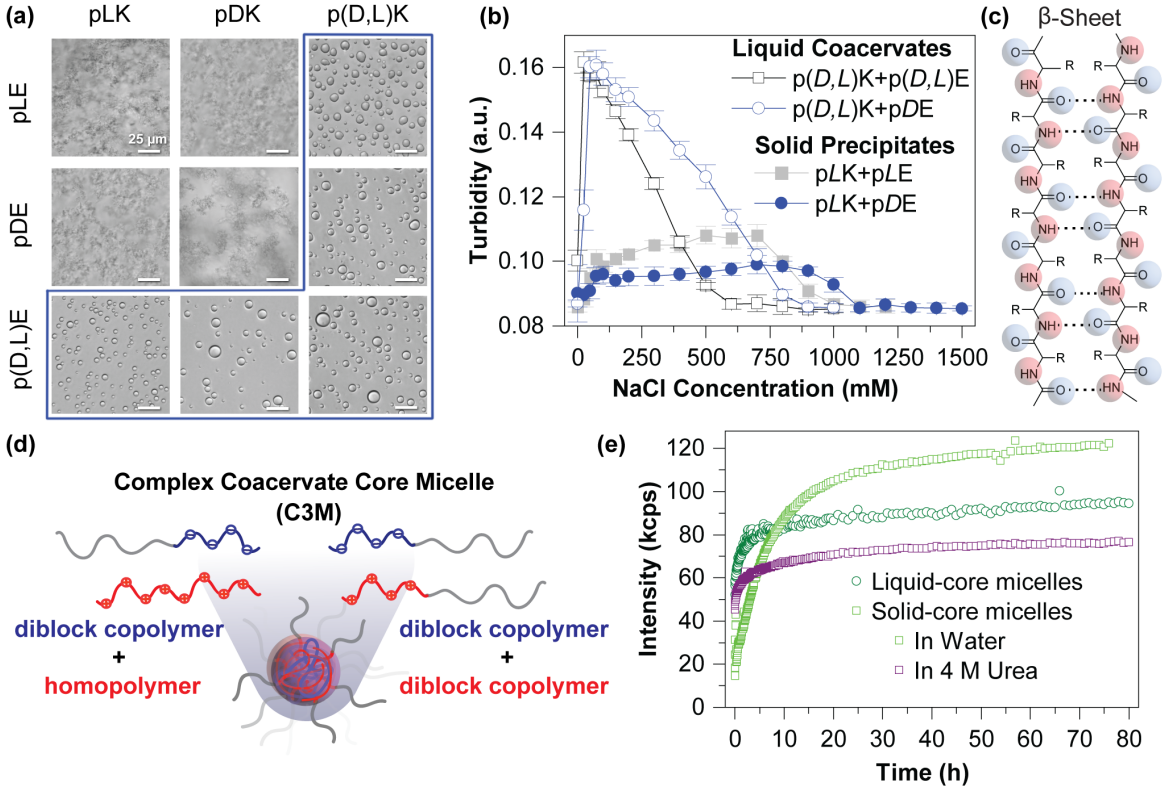

Figure 5: Chirality as a determinant for liquid vs. solid phase separation. (a) Optical micrographs showing liquid coacervates and solid precipitates as a function of chirality. **(b)** Turbidity vs. salt concentration for liquid coacervates and solid precipitates. **(c)** Schematic β-sheet structure. **(d)** Schematic of C3Ms formed from two oppositely-charged diblock copolymers or a diblock and a homopolymer. **(f)** Kinetics of micelle formation. The total scattered intensity as a function of time for liquid-core and solid-core micelles. Reproduced with permission from Ref 3. Copyright The Authors, some rights reserved; exclusive licensee Nature. Distributed under a Creative Commons Attribution License 4.0 (CC BY) https://creativecommons.org/licenses/by/4.0/.

While the solid vs. liquid nature of a macroscale complex is straightforward to observe, the same phenomena can also affect the formation of nanometer-scale complex coacervate core micelles (C3Ms). C3Ms form when at least one of the complexing species is a double

hydrophilic block copolymer, with the polyelectrolyte block coupled to a neutral, water-soluble polymer (Figure 5d).[51–54] Light scattering data examining the kinetics of micelle equilibration showed that liquid-core micelles formed using racemic polyglutamate equilibrated quickly, while homochiral polypeptides equilibrated more slowly, suggesting a solid core (Figure 5e).[3] Similar to bulk complexes, urea accelerated chain rearrangement, suggesting conversion from a solid β-sheet structure to a disordered liquid core.

While the initial studies looking into the effects of chirality used random copolypeptides of *D*- and *L*-amino acids, the potential for using chirality and hydrogen bonding as a method to control material properties raised the question of how many sequential homochiral amino acids were needed to stabilize β-sheet formation. A combination of experimental studies with sequence-controlled chirality[55] and molecular dynamics (MD) simulations[50] were conducted to answer this question. In both cases, a run of eight or more homochiral amino acids were needed to form a persistent β-sheet structure (Figure 6a).

These studies highlight ways that electrostatic interactions can work in parallel with orthogonal interactions. To date, efforts have largely focused on hydrogen bonding; however, interactions such as cation-π[29,30,56] and π-π[31,57] are known to be important in condensate formation, and other factors such as dipolar interactions, van der Waals forces, and stereocomplexation could also potentially be leveraged to tune assembly.

Polymer Architecture:

In addition to linear sequence effects, polymer architecture can also affect coacervation. Johnston *et al*., coupled a penta-lysine peptide to a polymerizable cyclooctene to create a comb-polymer architecture (Figure 6b)[58] analogous to glycosylated proteins such

as mucin.[59] The salt resistance of coacervates formed by complexing this comb polymer with a linear polyglutamate was nearly half the value measured for the linear system with an equivalent number of amino acids (Figure 6c). This loss in salt stability was expected because of the similar counterion condensation effects as described in Figure 2d. However, an interesting consequence of the comb architecture was that by maintaining the 'size' of the charged block, it became possible to dilute the overall charge density of the polymers with large amounts of a zwitterionic comonomer while minimally affecting the salt resistance (Figure 6c).

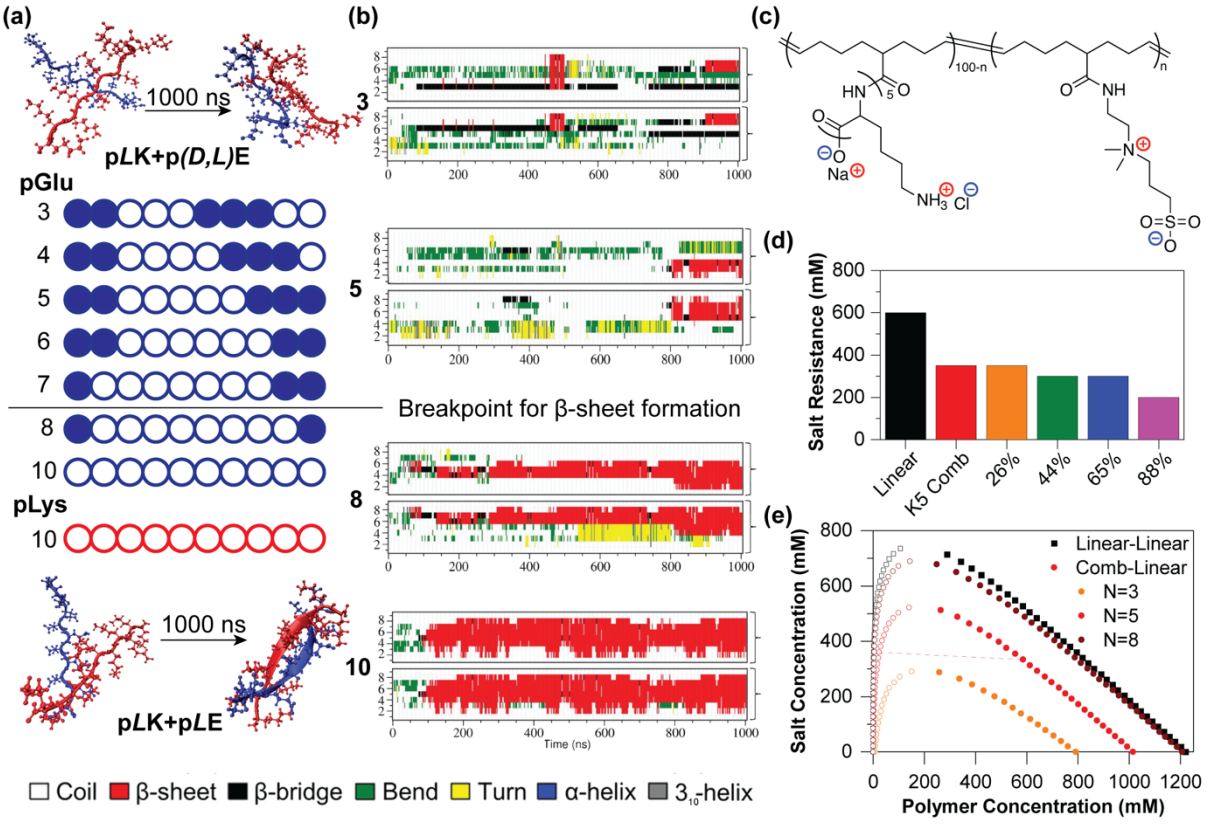

Figure 6: Effect of chiral sequence and polymer architecture on complex coacervation. (a) Simulation snapshots showing the time-evolution of secondary structure of a racemic poly(lysine)/poly(glutamic acid) complex that remains unstructured and a homochiral complex that forms a β-sheet. Schematic indicating the sequence progression of chirality explored, showing the breakpoint for β-sheet formation. Reproduced with permission from Ref 3. Copyright The Authors, some rights reserved; exclusive licensee Nature. Distributed under a Creative Commons Attribution License 4.0 (CC BY) https://creativecommons.org/licenses/by/4.0/. **(b)** Secondary structure for each residue vs. time for four of the systems shown in **(a)**. Reproduced from Ref. 50 with permission from the Royal Society of Chemistry. **(c)** Structure of a sulfobetaine-containing pentalysine comb polymer and **(d)** the corresponding plot of salt resistance as a function of polymer architecture and sulfobetaine content. **(e)** Simulated binodal curves showing the effect of comb-chain length compared to the linear-linear systems. Figure reproduced from Ref. 58 with permission from the Royal Society of Chemistry.

Simulations were also leveraged to understand the effect of comb architecture on coacervation.[58] In particular, simulations looked at the length of the polypeptide comb. Interestingly, a comb length of eight residues was sufficient to approach the phase behavior of a linear system with the same number of charges (Figure 6d). Building connections to simulation studies of sequence,[2] a run of eight charged amino acids was shown to create an environment in the middle of the block with the same tendency for ion pair formation as a homopolymer, which could explain this result. It is also intriguing that eight residues was the breakpoint for β-sheet formation via hydrogen bonding. However, further research would be needed to determine whether this length scale is universal or merely coincidental.

Encapsulation:

While IDPs have been implicated as the scaffold around which condensates form,[12,13,60] these compartments tend to host globular proteins, either for temporary storage as in the case of stress granules,[48] or to facilitate enzyme function.[9,61,62] This idea of selective encapsulation and potentially enhanced function has relevance beyond biology for applications in personal care, drug delivery, and biocatalysis.[63] Here again, polypeptide-based coacervates can be used to understand how sequence can enable selective enzyme enrichment and (potentially) enhance the stability and/or activity of guest proteins.

One unique aspect of polypeptide-based coacervates is their similarity to both condensates and the cytosol. While many 'traditional' biomolecule formulations involve relatively dilute solutions, the intracellular environment is very crowded.[22] Thus, coacervates have the potential to provide compartmentalization, physical crowding, and sequence-based modulation of the molecular environment.

Importantly, compartmentalization via coacervation should not be thought of as simple encapsulation, with the guest molecule playing no role in its incorporation. Complex coacervation relies on electrostatic interactions to drive self-assembly. Thus, the charge of a guest protein is critical in determining the extent to which it will partition into the coacervate. For example, Obermeyer and coworkers employed both chemical ligation and mutagenesis to engineer "supercharged" proteins to test the minimum charge levels required to facilitate coacervation between an anionic protein and a cationic polymer.[64,65] However, not all protein targets allow for supercharging. To circumvent this limitation, the use of a ternary system, where the protein is complexed with both cationic and anionic polymers, allows for the incorporation of even weakly charged proteins.[4,66–68]

Delving further into this approach, our group looked to establish design rules for protein incorporation, considering electrostatic parameters such as pH, salt concentration, and the net charge and charge density of both the polymers and the proteins involved.[4] Coacervates were made using poly(lysine) and poly(glutamate), and a comparison was made in terms of the partition coefficient, defined as the ratio of protein in the coacervate and supernatant phases.

The effect of protein charge was examined by varying pH. As would be expected for a charge-dominated process, protein partitioning increased as the relative difference between the solution pH and the isoelectric point (pI) of the protein increased (Figure 7e). It is noteworthy that the various proteins shown in Figure 7e do not partition to the same extent, despite showing similar trends as a function of pH. These differences are not explained when the net charge of the proteins is considered (Figure 7f, Table 1), though there does appear to be a correlation between partitioning and the |net charge| of the protein normalized by the

number of amino acids (Figure 7g). However, the differences in the slope of the data for bovine serum albumin (BSA), hemoglobin (Hb), and chymotrypsin (ChT), as compared with hen egg white lysozyme (HEWL) suggest that different mechanisms may dominate the incorporation of these proteins.

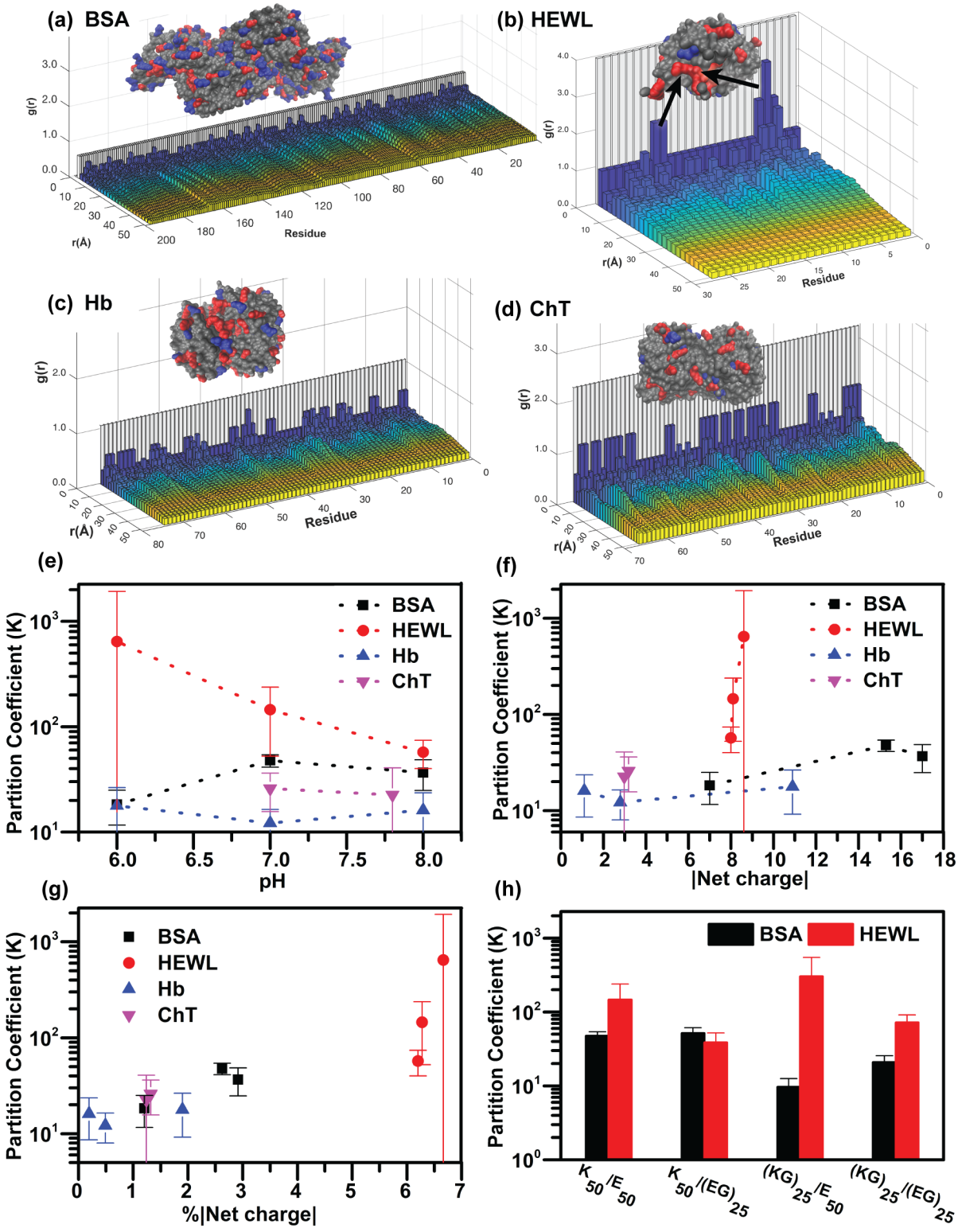

Figure 7: Incorporation of proteins into complex coacervates. Structural rendering of the proteins and 3D bar plot depictions of the single-molecule radial distribution function g(r) of the charged amino acids in **(a)** BSA, **(b)** HEWL, **(c)** Hb, and **(d)** ChT. The protein structures show the distribution of positive (red) and negative (blue) charges. The arrows in **(b)** indicate the presence of a charge patch. Plots of maximum partition coefficient as a function of **(e)** pH, **(f)** |net charge|, **(g)** |net charge|/total number of amino acids, and **(h)** charge density of the complexing peptides. The error bars are the standard deviation of replicate measurements, including propagated error. Data adapted from Refs. 4,69.

Table 1: Physical parameters for BSA, HEWL, Hb, and ChT.[4,69]

Protein		BSA	HEWL	Hb	ChT
MW (kDa)		66.4	14.3	64.5	25.0
# of Residues		583	129	574	241
pI		5.5	11.7	9.0	9.7
Net Charge	pH 6	-7.0	+8.6	+10.9	-
	pH 7	-15.3	+8.1	+2.8	+3.2
	pH 8	-17.0	+8.0	+1.1	-

Why then, would a change in the net charge of BSA by 10 result in a much smaller increase in protein partitioning than a shift of only 0.6 for HEWL? Similarly, why would ChT incorporate more strongly than Hb, despite having practically the same net charge? These questions can be answered by considering the distribution of charges on the surface of the proteins.[4] Figures 7a-d plot the radial distribution function g(r) for each of the ionizable residues within the various proteins, alongside a structural depiction highlighting the location of charged groups. While the analysis of BSA and Hb shows no significant correlations at short distances, a dramatic set of peaks is observed for HEWL, and some weaker correlations for ChT. We hypothesize that the presence of these clusters of charged residues help to drive protein partitioning in a more dramatic fashion than net charge alone.

A similar case for the importance of charge patterning can be made with respect to the coacervating polypeptides. While relatively strong partitioning was observed when fully charged homopoly(lysine) and homopoly(glutamate) were used, significant changes were observed when polypeptides with an alternating sequence of charged residues and glycine were used to decrease the charge density by half (Figure 7h). Using these polypeptides, we observed either an increase in protein partitioning if the net charge of the patterned polypeptide matched that of the protein (*i.e.*, competition between the protein and

polypeptide was decreased), or a decrease if the charge density of the polypeptide of opposite charge was decreased, meaning that the associations between polypeptide and protein were weakened.

Experimental factors external to the charge state of the proteins and polypeptides were also considered. Salt is known to screen electrostatic interactions and potentially disrupt coacervation. In fact, the amount of salt needed to dramatically reduce protein partitioning (Figure 8a) was far less than the amount needed to disassemble the overall coacervate.

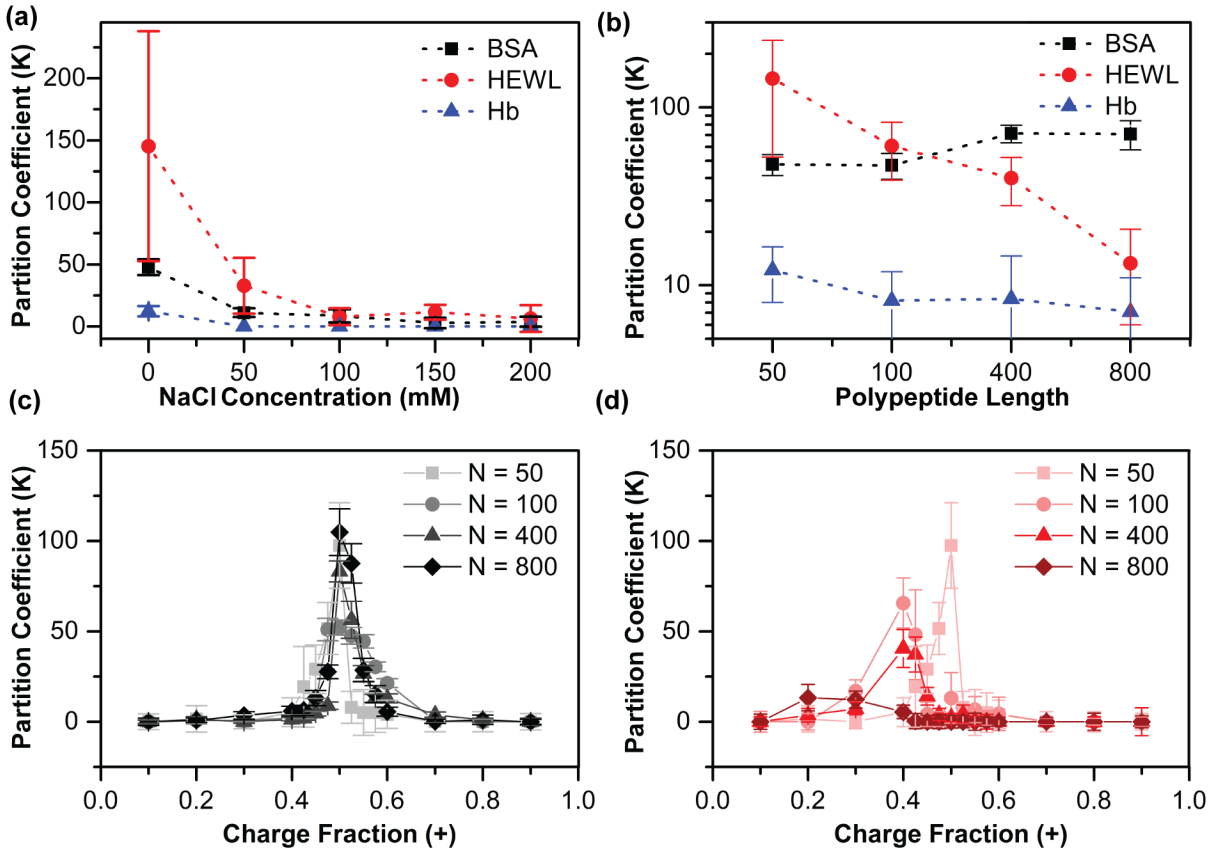

Figure 8: Effect of salt concentration and polypeptide length on protein incorporation. (a) Partition coefficient vs. NaCl concentration and **(b)** polypeptide length. Partition coefficient as a function of the cationic charge fraction of the polypeptide mixture used for coacervates of different polypeptide lengths with **(c)** BSA and **(d)** HEWL. Cationic charge fraction is defined on a monomer basis as $[lysine]/([lysine]+[glutamate])$. The error bars are the standard deviation of the reported average including propagated error. Data adapted from Ref. 4.

One purely physical consideration in formulating coacervates is the length of the polypeptides used. In terms of phase behavior, length has been shown to increase the size of the two-phase region,[70,71] as expected by theory.[24,72,73] However, the effect of polymer length

on the incorporation of proteins or other guest molecules appears to be very complex. Simple analysis of the maximum partitioning as a function of polypeptide length showed no clear trend across the different proteins (Figure 8b). However, a closer look at the underlying data showed interesting differences with regards to how the optimum coacervate composition changed with polypeptide length.

Figures 8c,d show how protein partitioning changed as a function of the relative amount of poly(lysine) or poly(glutamate) present. In the absence of protein, the maximum amount of coacervation is expected to occur at a 1:1 charge ratio, and in general this result shifted only slightly when protein was added to coacervates made with short polypeptides, and in a direction that could be explained based on the net charge of the protein.[4] However, while the location of this maximum coacervation remained near this charge neutral condition with increasing polypeptide length for BSA, a dramatic shift to lower charge fractions (*i.e.*, net negative compositions) was seen for HEWL (Figures 8c,d). While it might be possible that geometric arguments related to the size of the proteins could prove relevant, we hypothesize that this shift is due instead to the presence of the charge patch on HEWL.

We tested the potential effects of particle size by comparing the trends of encapsulation as a function of chain length for proteins[4] with those for viruses.[74] Specifically, porcine parvovirus (PPV) and human rhinovirus (HRV) were incorporated into the same poly(lysine)/poly(glutamate) coacervate system. Both viruses carry a net-negative charge and have significant charge patches on their surfaces (Figure 9a,b). Interestingly, the optimum charge ratio for coacervation with both viruses shifted towards net-negative charge fractions as the polypeptide chain length increased (Figure 9c,d). This trend was similar to that seen for HEWL, despite the net charge of HEWL being opposite that of the viruses. Additionally, while

both a shift and a decrease in partitioning for HEWL was observed with increasing chain length, no decrease in partitioning was observed for PPV, and an increase was observed for the longest polypeptide system with HRV. It is unclear whether these trends in encapsulation are a function of the degree of patchiness, or some other factor, and studies looking into these types of geometrical factors for both the globular 'guest' molecule and the coacervating polypeptides have the potential to reveal interesting physics underlying these types of systems.

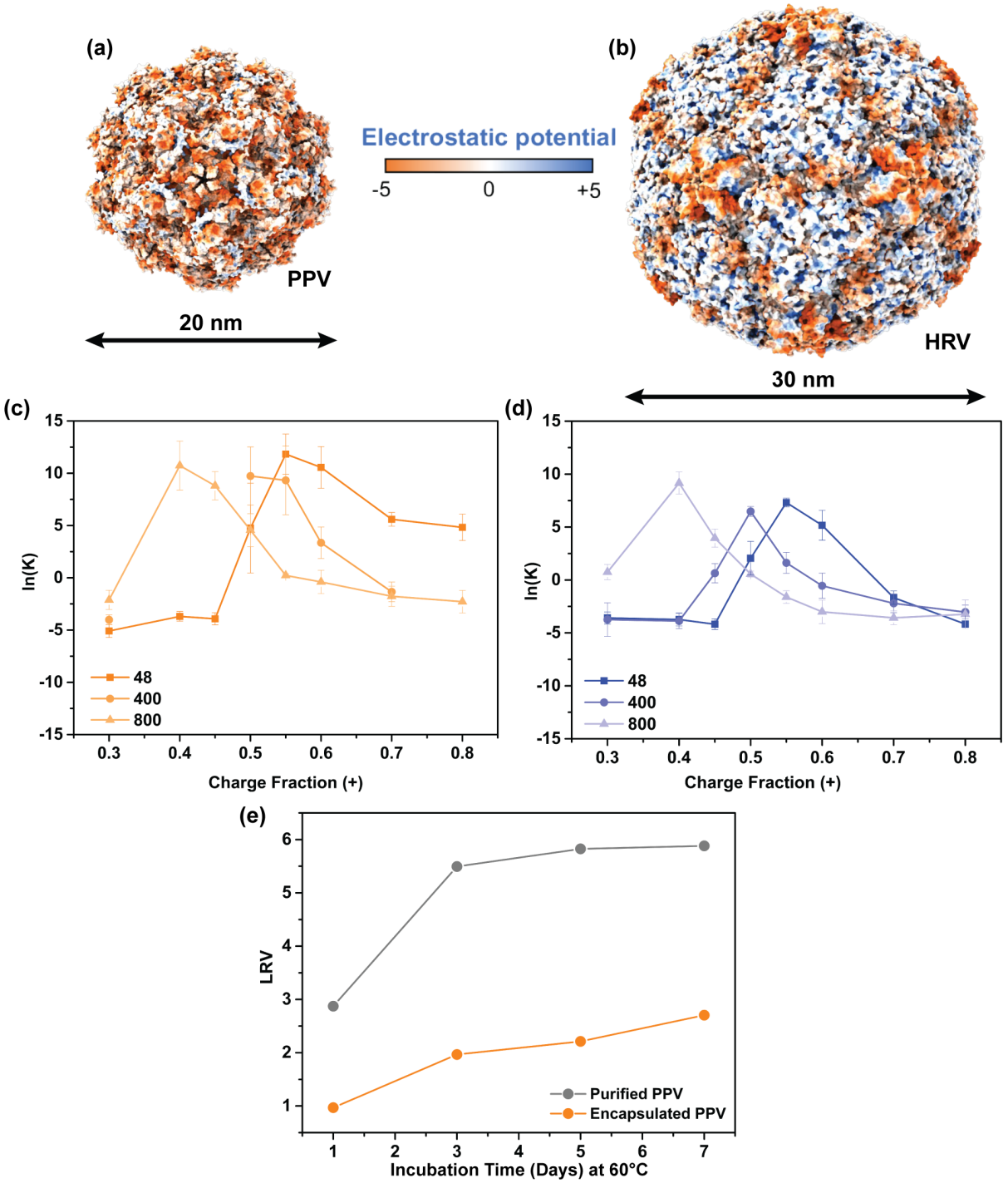

Figure 9: Virus incorporation and stabilization. Representation of the electrostatic potential on the **(a)** PPV and **(b)** HRV capsids. Partition coefficient ln(K) for **(c)** PPV and **(d)** HRV vs. the cationic charge fraction the polypeptide mixture used. Error bars represent the standard deviation from replicate measurements. Reprinted with permission from Ref. 74. Copyright 2023 American Chemical Society. **(e)** Thermal stability defined as the log reduction value (LRV) vs. time for free and encapsulated PPV. $LRV = -log(\frac{C_f}{C_i})$, where C_f is the final virus concentration after heat treatment, and C_i is the initial virus concentration. Data were adapted from Ref. 75.

While our discussion thus far has focused on simple partitioning of biomolecules into coacervates, one key motivation has been to improve the stability of these molecules.

Accelerated aging experiments were performed with PPV, comparing the titer for virus in solution vs. in coacervate (Figure 9e).[75] Very excitingly, a significant improvement in the stability of PPV was observed upon coacervation, and while the improvement was not sufficient for translation into an actual formulation, subsequent investigations into the effect of peptide chemistry have the potential to further enhance performance. Similar approaches could be leveraged to help purify and/or stabilize proteins or enzymes for applications ranging from medicine to sensors to biocatalysis, and this work is ongoing in our group.

Conclusions: Building Connections Between Synthetic Coacervates and Biological Condensates

Complex coacervates assembled from oppositely-charged polypeptides have allowed for fundamental studies that explore the ways in which sequence, chemical, and architectural interactions drive LLPS. These simplified approaches parallel efforts in the field of biological condensates, where the complexity of highly evolved living systems can both provide inspiration and create challenges. Ultimately, LLPS materials have the potential to enable a new generation of approaches to compartmentalization, purification, and biomolecule stabilization that could have implications from medicine to biocatalysis.

Acknowledgements:

This work was supported by the National Science Foundation (DMR-1945521, DMR-2118788), the National Institutes of Health (1R21AI150962-01) and the São Paulo Research Foundation FAPESP projects 2015/25406-5, 2021/12071-6, and scholarships to J.B.S. (2018/25041-5, 2020/11735-5, and 2021/11317-1).

Author Biographies:

Arvind Sathyavageeswaran completed his B.S. in Chemical Engineering at the Indian Institute of Technology Madras and is currently a PhD student at the University of

Massachusetts, Amherst. His research focuses on studying sequence effects in complex coacervation with the goal of encapsulating and stabilizing biologic materials.

Júlia Bonesso Sabadini obtained her B.Sc. from the University of São Paulo. Currently, she is a PhD student at the University of Campinas under the supervision of Profs. Loh and Perry. Her research focuses on understanding the encapsulation of proteins into coacervate micelles.

Sarah Perry is an Associate Professor of Chemical Engineering at the University of Massachusetts Amherst. She received her PhD in Chemical and Biomolecular Engineering from the University of Illinois at Urbana-Champaign and was a postdoctoral fellow at the University of California Berkeley and the University of Chicago. Her research is highly interdisciplinary, and utilizes self-assembly, molecular engineering, and microfluidic technologies to understand the fundamental principles behind materials design to inform solutions to real-world challenges.

References:

(1) Chang, L. W.; Lytle, T. K.; Radhakrishna, M.; Madinya, J. J.; Vélez, J.; Sing, C. E.; Perry, S. L. Sequence and Entropy-Based Control of Complex Coacervates. *Nat Commun* **2017**, *8*, 1273. https://doi.org/10.1038/s41467-017-01249-1.

(2) Lytle, T. K.; Chang, L. W.; Markiewicz, N.; Perry, S. L.; Sing, C. E. Designing Electrostatic Interactions via Polyelectrolyte Monomer Sequence. *ACS Cent Sci* **2019**, *5*, 709–718. https://doi.org/10.1021/acscentsci.9b00087.

(3) Perry, S. L.; Leon, L.; Hoffmann, K. Q.; Kade, M. J.; Priftis, D.; Black, K. A.; Wong, D.; Klein, R. A.; Pierce, C. F.; Margossian, K. O.; Whitmer, J. K.; Qin, J.; de Pablo, J. J.; Tirrell, M. Chirality-Selected Phase Behaviour in Ionic Polypeptide Complexes. *Nat Commun* **2015**, *6*, 6052. https://doi.org/10.1038/ncomms7052.

(4) Blocher McTigue, W. C.; Perry, S. L. Design Rules for Encapsulating Proteins into Complex Coacervates. *Soft Matter* **2019**, *15*, 3089–3103. https://doi.org/10.1039/C9SM00372J.

(5) Brangwynne, C. P.; Eckmann, C. R.; Courson, D. S.; Rybarska, A.; Hoege, C.; Gharakhani, J.; Jülicher, F.; Hyman, A. A. Germline P Granules Are Liquid Droplets That Localize by Controlled Dissolution/Condensation. *Science (1979)* **2009**, *324*, 1729–1732. https://doi.org/10.1126/science.1172046.

(6) Zhu, L.; Brangwynne, C. P. Nuclear Bodies: The Emerging Biophysics of Nucleoplasmic Phases. *Curr Opin Cell Biol* **2015**, *34*, 23–30. https://doi.org/10.1016/j.ceb.2015.04.003.

(7) Elbaum-Garfinkle, S.; Kim, Y.; Szczepaniak, K.; Chen, C. C. H.; Eckmann, C. R.; Myong, S.; Brangwynne, C. P. The Disordered P Granule Protein LAF-1 Drives Phase Separation into Droplets with Tunable Viscosity and Dynamics. *Proc Natl Acad Sci U S A* **2015**, *112*, 7189–7194. https://doi.org/10.1073/pnas.1504822112.

(8) Hyman, A. A.; Weber, C. A.; Jülicher, F. Liquid-Liquid Phase Separation in Biology. *Annu Rev Cell Dev Biol* **2014**, *30*, 39–58. https://doi.org/10.1146/annurev-cellbio-100913-013325.

(9) Shin, Y.; Brangwynne, C. P. Liquid Phase Condensation in Cell Physiology and Disease. *Science (1979)* **2017**, *357*, eaaf4382. https://doi.org/10.1126/science.aaf4382.

(10) Weber, S. C.; Brangwynne, C. P. Getting RNA and Protein in Phase. *Cell* **2012**, *149*, 1188–1191. https://doi.org/10.1016/j.cell.2012.05.022.

(11) Brangwynne, C. P.; Tompa, P.; Pappu, R. V. Polymer Physics of Intracellular Phase Transitions. *Nat Phys* **2015**, *11*, 899–904. https://doi.org/10.1038/nphys3532.

(12) Perry, S. L. Phase Separation: Bridging Polymer Physics and Biology. *Curr Opin Colloid Interface Sci* **2019**, *39*, 86–97. https://doi.org/10.1016/j.cocis.2019.01.007.

(13) Forman-Kay, J. D.; Mittag, T. From Sequence and Forces to Structure, Function, and Evolution of Intrinsically Disordered Proteins. *Structure* **2013**, *21*, 1492–1499. https://doi.org/10.1016/j.str.2013.08.001.

(14) Uversky, V. N.; Kuznetsova, I. M.; Turoverov, K. K.; Zaslavsky, B. Intrinsically Disordered Proteins as Crucial Constituents of Cellular Aqueous Two Phase Systems and Coacervates. *FEBS Lett* **2015**, *589*, 15–22. https://doi.org/10.1016/j.febslet.2014.11.028.

(15) Nott, T. J.; Petsalaki, E.; Farber, P.; Jervis, D.; Fussner, E.; Plochowietz, A.; Craggs, T. D.; Bazett-Jones, D. P.; Pawson, T.; Forman-Kay, J. D.; Baldwin, A. J. Phase Transition of a Disordered Nuage Protein Generates Environmentally Responsive Membraneless Organelles. *Mol Cell* **2015**, *57*, 936–947. https://doi.org/10.1016/j.molcel.2015.01.013.

(16) Lee, C. F.; Brangwynne, C. P.; Gharakhani, J.; Hyman, A. A.; Jülicher, F. Spatial Organization of the Cell Cytoplasm by Position-Dependent Phase Separation. *Phys Rev Lett* **2013**, *111*. https://doi.org/10.1103/PhysRevLett.111.088101.

(17) Perillo, M. A.; Burgos, I.; Clop, E. M.; Sanchez, J. M.; Nolan, V. The Role of Water in Reactions Catalysed by Hydrolases under Conditions of Molecular Crowding. *Biophys Rev* **2023**, *15*, 639–660. https://doi.org/10.1007/s12551-023-01104-2.

(18) Fu, J.; Schlenoff, J. B. Driving Forces for Oppositely Charged Polyion Association in Aqueous Solutions: Enthalpic, Entropic, but Not Electrostatic. *J Am Chem Soc* **2016**, *138*, 980–990. https://doi.org/10.1021/jacs.5b11878.

(19) Sadman, K.; Wang, Q.; Chen, Y.; Keshavarz, B.; Jiang, Z.; Shull, K. R. Influence of Hydrophobicity on Polyelectrolyte Complexation. *Macromolecules* **2017**, *50*, 9417–9426. https://doi.org/10.1021/acs.macromol.7b02031.

(20) Yang, M.; Sonawane, S. L.; Digby, Z. A.; Park, J. G.; Schlenoff, J. B. Influence of "Hydrophobicity" on the Composition and Dynamics of Polyelectrolyte Complex Coacervates. *Macromolecules* **2022**, *55*, 7594–7604. https://doi.org/10.1021/acs.macromol.2c00267.

(21) Chen, S.; Wang, Z. G. Driving Force and Pathway in Polyelectrolyte Complex Coacervation. *Proc Natl Acad Sci U S A* **2022**, *119*, e2209975119. https://doi.org/10.1073/pnas.2209975119.

(22) Fulton, A. B. How Crowded Is the Cytoplasm? *Cell* **1982**, *30*, 345–347. https://doi.org/10.1016/0092-8674(82)90231-8.

(23) Li, L.; Srivastava, S.; Andreev, M.; Marciel, A. B.; de Pablo, J. J.; Tirrell, M. V. Phase Behavior and Salt Partitioning in Polyelectrolyte Complex Coacervates. *Macromolecules* **2018**, *51*, 2988–2995. https://doi.org/10.1021/acs.macromol.8b00238.

(24) Sing, C. E.; Perry, S. L. Recent Progress in the Science of Complex Coacervation. *Soft Matter* **2020**, *16*, 2885–2914. https://doi.org/10.1039/d0sm00001a.

(25) Amblard, M.; Fehrentz, J. A.; Martinez, J.; Subra, G. Methods and Protocols of Modern Solid Phase Peptide Synthesis. *Mol Biotechnol* **2006**, *33*, 239–254. https://doi.org/10.1385/MB:33:3:239.

(26) Merrifield, R. B. Solid-Phase Peptide Synthesis; Nord, F. F., Series Ed.; Advances in Enzymology - and Related Areas of Molecular Biology; **1969**. https://doi.org/10.1002/9780470122778.ch6.

(27) Rumyantsev, A. M.; Jackson, N. E.; Yu, B.; Ting, J. M.; Chen, W.; Tirrell, M. V.; de Pablo, J. J. Controlling Complex Coacervation via Random Polyelectrolyte Sequences. *ACS Macro Lett* **2019**, *8*, 1296–1302. https://doi.org/10.1021/acsmacrolett.9b00494.

(28) Tabandeh, S.; Lemus, C. E.; Leon, L. Deciphering the Role of π-Interactions in Polyelectrolyte Complexes Using Rationally Designed Peptides. *Polymers (Basel)* **2021**, *13*, 2074. https://doi.org/10.3390/polym13132074.

(29) Lu, Q.; Oh, D. X.; Lee, Y.; Jho, Y.; Hwang, D. S.; Zeng, H. Nanomechanics of Cation-π Interactions in Aqueous Solution. *Angewandte Chemie - International Edition* **2013**, *52*, 3944–3948. https://doi.org/10.1002/anie.201210365.

(30) Dougherty, D. A. The Cation-π Interaction. *Acc Chem Res* **2013**, *46*, 885–893. https://doi.org/10.1021/ar300265y.

(31) Hunter, C. A.; Singh, J.; Thornton, J. M. Π-Π Interactions: The Geometry and Energetics of Phenylalanine-Phenylalanine Interactions in Proteins. *J Mol Biol* **1991**, *218*, 837–846. https://doi.org/10.1016/0022-2836(91)90271-7.

(32) Perry, S. L.; Sing, C. E. 100th Anniversary of Macromolecular Science Viewpoint: Opportunities in the Physics of Sequence-Defined Polymers. *ACS Macro Lett* **2020**, *9*, 216–225. https://doi.org/10.1021/acsmacrolett.0c00002.

(33) AlQuraishi, M. Machine Learning in Protein Structure Prediction. *Curr Opin Chem Biol* **2021**, *65*, 1–8. https://doi.org/10.1016/j.cbpa.2021.04.005.

(34) Martin, E. W.; Mittag, T. Relationship of Sequence and Phase Separation in Protein Low-Complexity Regions. Biochemistry **2018**, *57*, 2478–2487. https://doi.org/10.1021/acs.biochem.8b00008.

(35) Das, R. K.; Pappu, R. V. Conformations of Intrinsically Disordered Proteins Are Influenced by Linear Sequence Distributions of Oppositely Charged Residues. *Proc Natl Acad Sci U S A* **2013**, *110*, 13392–13397. https://doi.org/10.1073/pnas.1304749110.

(36) Pak, C. W.; Kosno, M.; Holehouse, A. S.; Liu, D. R.; Pappu, R. V; Rosen, M. K.; Pak, C. W.; Kosno, M.; Holehouse, A. S.; Padrick, S. B.; Mittal, A.; Ali, R.; Yunus, A. A. Sequence Determinants of Intracellular Phase Separation by Complex Coacervation of a Disordered Article Sequence Determinants of Intracellular Phase Separation by Complex Coacervation of a Disordered Protein. *Mol Cell* **2016**, *63*, 72–85. https://doi.org/10.1016/j.molcel.2016.05.042.

(37) Priftis, D.; Laugel, N.; Tirrell, M. Thermodynamic Characterization of Polypeptide Complex Coacervation. *Langmuir* **2012**, *28*, 15947–15957. https://doi.org/10.1021/la302729r.

(38) Ou, Z.; Muthukumar, M. Entropy and Enthalpy of Polyelectrolyte Complexation: Langevin Dynamics Simulations. *Journal of Chemical Physics* **2006**, *124*, 154902. https://doi.org/10.1063/1.2178803.

(39) Manning, G. S. Limiting Laws and Counterion Condensation in Polyelectrolyte Solutions. 7. Electrophoretic Mobility and Conductance. *Journal of Physical Chemistry* **1981**, *85*, 1506–1515. https://doi.org/10.1021/j150611a011.

(40) Manning, G. S. Limiting Laws and Counterion Condensation in Polyelectrolyte Solutions I. Colligative Properties. *J Chem Phys* **1969**, *51*, 924–933. https://doi.org/10.1063/1.1672157.

(41) Dinic, J.; Marciel, A. B.; Tirrell, M. V. Polyampholyte Physics: Liquid–Liquid Phase Separation and Biological Condensates. *Curr Opin Colloid Interface Sci* **2021**, *54*, 101457. https://doi.org/10.1016/j.cocis.2021.101457.

(42) Madinya, J. J.; Chang, L. W.; Perry, S. L.; Sing, C. E. Sequence-Dependent Self-Coacervation in High Charge-Density Polyampholytes. *Mol Syst Des Eng* **2020**, *5*, 632–644. https://doi.org/10.1039/c9me00074g.

(43) Tabandeh, S.; Leon, L. Engineering Peptide-Based Polyelectrolyte Complexes with Increased Hydrophobicity. *Molecules* **2019**, *24*, 868. https://doi.org/10.3390/molecules24050868.

(44) Schlenoff, J. B.; Rmaile, A. H.; Bucur, C. B. Hydration Contributions to Association in Polyelectrolyte Multilayers and Complexes: Visualizing Hydrophobicity. *J Am Chem Soc* **2008**, *130*, 13589–13597. https://doi.org/10.1021/ja802054k.

(45) Huang, J.; Laaser, J. E. Charge Density and Hydrophobicity-Dominated Regimes in the Phase Behavior of Complex Coacervates. *ACS Macro Lett* **2021**, *10*, 1029–1034. https://doi.org/10.1021/acsmacrolett.1c00382.

(46) Israelachvili, J. *Intermolecular and Surface Forces*, Third.; Academic Press, 2011. https://doi.org/10.1016/b978-0-12-391927-4.10024-6.

(47) Perry, S. L.; Li, Y.; Priftis, D.; Leon, L.; Tirrell, M. The Effect of Salt on the Complex Coacervation of Vinyl Polyelectrolytes. *Polymers (Basel)* **2014**, *6*, 1756–1772. https://doi.org/10.3390/polym6061756.

(48) Banani, S. F.; Lee, H. O.; Hyman, A. A.; Rosen, M. K. Biomolecular Condensates: Organizers of Cellular Biochemistry. *Nat Rev Mol Cell Biol* **2017**, *18*, 285–298. https://doi.org/10.1038/nrm.2017.7.

(49) Han, T. W.; Kato, M.; Xie, S.; Wu, L. C.; Mirzaei, H.; Pei, J.; Chen, M.; Xie, Y.; Allen, J.; Xiao, G.; McKnight, S. L. Cell-Free Formation of RNA Granules: Bound RNAs Identify Features and Components of Cellular Assemblies. *Cell* **2012**, *149*, 768–779. https://doi.org/10.1016/j.cell.2012.04.016.

(50) Hoffmann, K. Q.; Perry, S. L.; Leon, L.; Priftis, D.; Tirrell, M.; de Pablo, J. J. A Molecular View of the Role of Chirality in Charge-Driven Polypeptide Complexation. *Soft Matter* **2015**, *11*, 1525–1538. https://doi.org/10.1039/c4sm02336f.

(51) Voets, I. K.; de Keizer, A.; Cohen Stuart, M. A. Complex Coacervate Core Micelles. *Adv Colloid Interface Sci* **2009**, *147–148*, 300–318. https://doi.org/10.1016/j.cis.2008.09.012.

(52) Spruijt, E.; Sprakel, J.; Cohen Stuart, M. A.; Van Der Gucht, J. Interfacial Tension between a Complex Coacervate Phase and Its Coexisting Aqueous Phase. *Soft Matter* **2009**, *6*, 172–178. https://doi.org/10.1039/b911541b.

(53) Lindhoud, S.; Voorhaar, L.; Vries, R. De; Schweins, R.; Cohen Stuart, M. A.; Norde, W. Salt-Induced Disintegration of Lysozyme-Containing Polyelectrolyte Complex Micelles. *Langmuir* **2009**, *25*, 11425–11430. https://doi.org/10.1021/la901591p.

(54) Kim, A.; Miura, Y.; Ishii, T.; Mutaf, O. F.; Nishiyama, N.; Cabral, H.; Kataoka, K. Intracellular Delivery of Charge-Converted Monoclonal Antibodies by Combinatorial Design of Block/Homo Polyion Complex Micelles. *Biomacromolecules* **2016**, *17*, 446–453. https://doi.org/10.1021/acs.biomac.5b01335.

(55) Pacalin, N. M.; Leon, L.; Tirrell, M. Directing the Phase Behavior of Polyelectrolyte Complexes Using Chiral Patterned Peptides. *European Physical Journal: Special Topics* **2016**, *225*, 1805–1815. https://doi.org/10.1140/epjst/e2016-60149-6.

(56) Dougherty, D. A. Cation-π Interactions Involving Aromatic Amino Acids. *Journal of Nutrition* **2007**, *137*, 1504S-1508S. https://doi.org/10.1093/jn/137.6.1504s.

(57) Murthy, A. C.; Dignon, G. L.; Kan, Y.; Zerze, G. H.; Parekh, S. H.; Mittal, J.; Fawzi, N. L. Molecular Interactions Underlying Liquid–liquid Phase Separation of the FUS Low-Complexity Domain. *Nat Struct Mol Biol* **2019**, *26*, 637–648. https://doi.org/10.1038/s41594-019-0250-x.

(58) Johnston, B. M.; Johnston, C. W.; Letteri, R. A.; Lytle, T. K.; Sing, C. E.; Emrick, T.; Perry, S. L. The Effect of Comb Architecture on Complex Coacervation. *Org Biomol Chem* **2017**, *15*, 7630–7642. https://doi.org/10.1039/c7ob01314k.

(59) Davies, H. S.; Singh, P.; Deckert-Gaudig, T.; Deckert, V.; Rousseau, K.; Ridley, C. E.; Dowd, S. E.; Doig, A. J.; Pudney, P. D. A.; Thornton, D. J.; Blanch, E. W. Secondary Structure and Glycosylation of Mucus Glycoproteins by Raman Spectroscopies. *Anal Chem* **2016**, *88*, 11609–11615. https://doi.org/10.1021/acs.analchem.6b03095.

(60) Wright, P. E.; Dyson, H. J. Intrinsically Disordered Proteins in Cellular Signalling and Regulation. *Nat Rev Mol Cell Biol* **2015**, *16*, 18–29. https://doi.org/10.1038/nrm3920.

(61) Sweatt,S.K, Gower, B.A, Chieh, A.Y, Liu, Y, Li, L. Phase Transitions in the Assembly of Multi-Valent Signaling Proteins. *Physiol Behav* **2016**, *176*, 139–148. https://doi.org/10.1038/nature10879.Phase.

(62) Wang, Y.; Sarkar, M.; Smith, A. E.; Krois, A. S.; Pielak, G. J. Macromolecular Crowding and Protein Stability. *J Am Chem Soc* **2012**, *134*, 16614–16618. https://doi.org/10.1021/ja305300m.

(63) Blocher, W. C.; Perry, S. L. Complex Coacervate-Based Materials for Biomedicine. *Wiley Interdiscip Rev Nanomed Nanobiotechnol* **2017**, *9*, 76–78. https://doi.org/10.1002/wnan.1442.

(64) Obermeyer, A. C.; Mills, C. E.; Dong, X. H.; Flores, R. J.; Olsen, B. D. Complex Coacervation of Supercharged Proteins with Polyelectrolytes. *Soft Matter* **2016**, *12*, 3570–3581. https://doi.org/10.1039/c6sm00002a.

(65) Kim, S.; Sureka, H. V.; Kayitmazer, A. B.; Wang, G.; Swan, J. W.; Olsen, B. D. Effect of Protein Surface Charge Distribution on Protein-Polyelectrolyte Complexation. *Biomacromolecules* **2020**, *21*, 3026–3037. https://doi.org/10.1021/acs.biomac.0c00346.

(66) Van Lente, J. J.; Claessens, M. M. A. E.; Lindhoud, S. Charge-Based Separation of Proteins Using Polyelectrolyte Complexes as Models for Membraneless Organelles. *Biomacromolecules* **2019**, *20*, 3696–3703. https://doi.org/10.1021/acs.biomac.9b00701.

(67) Black, K. A.; Priftis, D.; Perry, S. L.; Yip, J.; Byun, W. Y.; Tirrell, M. Protein Encapsulation via Polypeptide Complex Coacervation. *ACS Macro Lett* **2014**, *3*, 1088–1091. https://doi.org/10.1021/mz500529v.

(68) Nolles, A.; Westphal, A. H.; De Hoop, J. A.; Fokkink, R. G.; Kleijn, J. M.; Van Berkel, W. J. H.; Borst, J. W. Encapsulation of GFP in Complex Coacervate Core Micelles. *Biomacromolecules* **2015**, *16*, 1542–1549. https://doi.org/10.1021/acs.biomac.5b00092.

(69) Sun, Y. Cryptic Materials and Coacervates, University of Massachusetts, Amherst, 2021.

(70) Li, L.; Rumyantsev, A. M.; Srivastava, S.; Meng, S.; de Pablo, J. J.; Tirrell, M. V. Effect of Solvent Quality on the Phase Behavior of Polyelectrolyte Complexes. *Macromolecules* **2021**, *54*, 105–114. https://doi.org/10.1021/acs.macromol.0c01000.

(71) Priftis, D.; Tirrell, M. Phase Behaviour and Complex Coacervation of Aqueous Polypeptide Solutions. *Soft Matter* **2012**, *8*, 9396–9405. https://doi.org/10.1039/c2sm25604e.

(72) Qin, J.; Priftis, D.; Farina, R.; Perry, S. L.; Leon, L.; Whitmer, J.; Hoffmann, K.; Tirrell, M.; de Pablo, J. J. Interfacial Tension of Polyelectrolyte Complex Coacervate Phases. *ACS Macro Lett* **2014**, *3*, 565–568. https://doi.org/10.1021/mz500190w.

(73) Spruijt, E.; Westphal, A. H.; Borst, J. W.; Cohen Stuart, M. A.; Van Der Gucht, J. Binodal Compositions of Polyelectrolyte Complexes. *Macromolecules* **2010**, *43*, 6476–6484. https://doi.org/10.1021/ma101031t.

(74) Joshi, P.U.; Decker, C.; Zeng, X.; Sathyavageeswaran, A.; Perry, S.L.; Heldt, C.L. Design Rules for the Sequestration of Viruses into Polypeptide Complex Coacervates. *Biomacromolecules* **2023**, ASAP. https://doi.org/10.1021/acs.biomac.3c00938

(75) Mi, X.; Blocher McTigue, W. C.; Joshi, P. U.; Bunker, M. K.; Heldt, C. L.; Perry, S. L. Thermostabilization of Viruses: Via Complex Coacervation. *Biomater Sci* **2020**, *8*, 7082–7092. https://doi.org/10.1039/d0bm01433h.